ELSEVIER

Biophysical Chemistry 101–102 (2002) 485–495

Biophysical Chemistry

www.elsevier.com/locate/bpc

Maximum-entropy calculation of free energy distributions in tRNAs

Douglas Poland*

Department of Chemistry, The Johns Hopkins University, Baltimore, MD 21218, USA

Received 8 August 2001; received in revised form 12 December 2001; accepted 12 December 2001

Abstract

We have previously shown that the distribution function describing the probability that a biological macromolecule picked at random has a particular enthalpy value can be calculated from the temperature dependence of the heat capacity of the macromolecule. The free energy as a function of enthalpy (free energy distribution) can then be determined from the enthalpy probability distribution. In addition, the free energy distribution at an arbitrary temperature can be calculated from the free energy distribution at a reference temperature. Here we apply this approach to a family of similar macromolecules, namely a set of transfer RNAs, specifically $tRNA^{Phe}$, $tRNA^{Val}$, $tRNA^{Met}$, $tRNA^{Ser}$, $tRNA^{Asp}$ and $tRNA^{Ile}$. Using published heat-capacity data, we calculate the enthalpy probability distribution functions for all of these molecules at five different temperatures covering the range from 30 to 80 °C. We then use these distributions to give a reference free-energy distribution, from which the thermodynamics at any temperature can be calculated for each species. We compare the reference free-energy distribution for the five tRNAs and find that, while the overall form of the distributions is similar, the local behavior of the functions varies considerably between the species.
© 2002 Elsevier Science B.V. All rights reserved.

Keywords: Enthalpy distribution; Heat capacity; Enthalpy moments; Maximum-entropy method; Free energy distribution

1. Introduction

Biological macromolecules in an aqueous solution exhibit a wide range of different enthalpy values. The quantitative description of this variation is the enthalpy distribution function, which gives the probability that a molecule picked at random will have a particular value of the enthalpy. We have recently shown [1] that if the experimental temperature variation of the heat capacity of a macromolecule is known, these data can then be converted into a set of moments of the enthalpy distribution function, and that the moments, using the maximum-entropy method, can be used to calculate the enthalpy probability distribution itself. We have applied this method to various proteins [2] using the heat capacity data of Makhatadze and Privalov [3]. The most interesting feature of these probability distributions is that for many proteins they are bimodal, with a peak at low enthalpy (representing the native state) and a peak at higher enthalpy (representing the denatured state). Thus, for some proteins the temperature

*Tel.: +1-410-516-7441; fax: +1-410-516-8420.
E-mail address: poland@jhunix.hcf.jhu.edu (D. Poland).

0301-4622/02/$ - see front matter © 2002 Elsevier Science B.V. All rights reserved.
PII: S0301-4622(02)00161-8

dependence of the heat capacity leads to a bimodal distribution function, supporting the two-state picture of protein denaturation (with broad fluctuations in the enthalpy of both native and denatured forms). A significant feature of this analysis is that no model is assumed: the two-state picture naturally emerges from the experimental heat-capacity data.

We then extended this kind of analysis to obtain the free energy corresponding to a particular enthalpy state, which was shown to be equivalent to an empirical method for calculating the density of states as a function of enthalpy [4]. An important property of the free energy as a function of enthalpy is that this distribution function can be obtained at any temperature by a simple modification to the free-energy distribution at a reference temperature. Thus, this reference free-energy distribution contains all of the thermodynamics of the macromolecule at any temperature. We have recently applied these ideas to the denaturation of proteins [5].

In the present paper we apply this method to a set of tRNA molecules with the purpose of comparing the free-energy distributions for a set of similar molecules. The data we use are those of Privalov and Filimonov [6], who have measured the heat capacity, $C_p(T)$, for the tRNA molecules for the amino acids valine, phenylalanine, methionine, isoleucine, serine and aspartic acid at various salt conditions. We copied and enlarged their published curves (contained [6] in their Fig. 1) and then computer-interpolated smooth curves through a large set of data points. The results for $tRNA^{Phe}$ are shown in Fig. 1. The three curves correspond to different salt conditions: the low curve is for 150 mM NaCl; the middle curve is for 150 mM NaCl and 1 mM $MgCl_2$; and the high curve is for 1 mM $MgCl_2$. There are similar data for the other five species. In the present paper we focus on the broadest curves (for 150 mM NaCl), both because we can obtain these data accurately from the published graphs and because we want to examine the behavior of the free-energy distribution for these molecules over a wide range of temperature. In the final section of this paper we treat the intermediate peak for $tRNA^{Phe}$ given in Fig. 1.

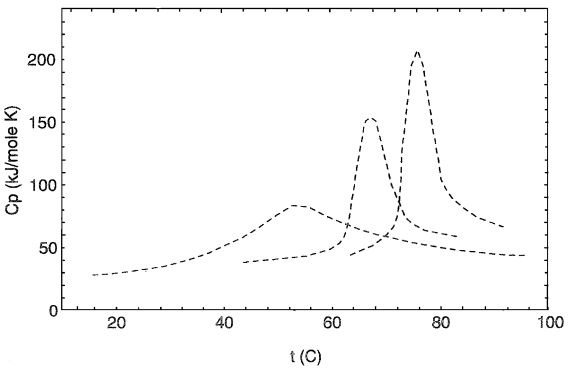

Fig. 1. The heat capacity in units of kJ mol^{-1} K^{-1} vs. the centigrade temperature for $tRNA^{Phe}$. The data are taken from Privalov and Filimonov [6]. The three curves are for different salt conditions: the low, broad curve is for the case of 150 mM NaCl; the middle curve is for the case of 150 mM NaCl and 1 mM $MgCl_2$; and the high curve is for the case of 1 mM $MgCl_2$.

The broad $C_p(T)$ curves for all six tRNA molecules (expressed in kJ mol^{-1} K^{-1} using the molecular weights in [6]) are shown in Fig. 2. The solid dots indicate the values of the temperature about which we form expansions of the heat capacity to obtain the enthalpy probability distributions. We outline this procedure in the next section.

2. Enthalpy probability distributions

The starting point for our free energy calculation is the experimental temperature dependence of the heat capacity, as shown in Fig. 2. A particular value of the temperature is picked, such as any one of the solid dots in Fig. 2, as an expansion center. Designating this reference temperature as T_r, we define ΔT as the difference between a general temperature T and T_r:

$$\Delta T = T - T_r \tag{1}$$

The temperature variation of the heat capacity in the neighborhood of T_r is then fitted to a series in powers of ΔT [the Taylor series expansion of $C_p(T)$ in terms of ΔT]:

$$C_p(T) = a + b\Delta T + c\Delta T^2 + \ldots \tag{2}$$

where

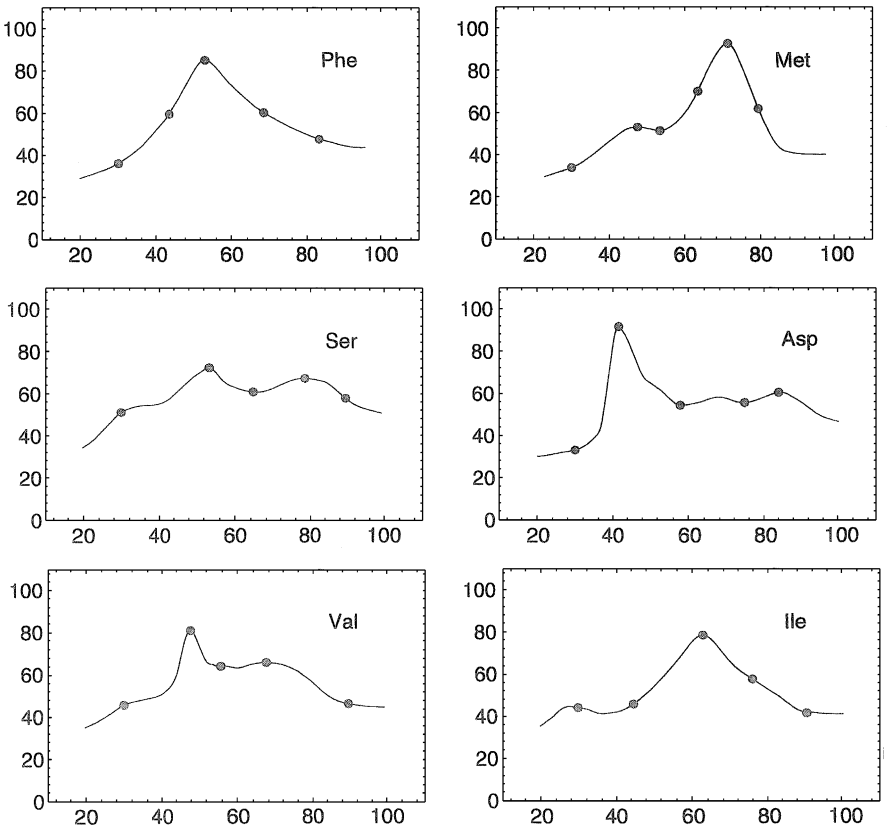

Fig. 2. The heat capacity in units of kJ mol^{-1} K^{-1} vs. the centigrade temperature for the tRNAs for phenyalanine, methionine, serine, aspartic acid, valine and isoleucine. The conditions are for the case of 150 mM NaCl, the conditions corresponding to the broad curve shown in Fig. 1. The solid dots indicate the temperatures about which expansions have been made.

$$a = C_p(T_r); \quad b = \left(\partial C_p/\partial T\right)_{T_r};$$
$$c = \frac{1}{2}\left(\partial^2 C_p/\partial T^2\right)_{T_r} \tag{3}$$

The series given in Eq. (2) is truncated at a finite number of terms. In particular, obtaining C_p through the quadratic term in ΔT is straightforward.

Using some elementary statistical mechanics, we can show [1] that the temperature derivatives of the heat capacity given in Eq. (3) are related to the moments of the enthalpy distribution. We define $P(H)$ as the normalized enthalpy distribution for a given temperature, which is the probability that a molecule picked at random has an enthalpy H. The first two moments of this distribution are:

$$H_1 = \int H\, P(H)\mathrm{d}H, \quad H_2 = \int H^2 P(H)\mathrm{d}H \tag{4}$$

with the mth moment being given by:

$$H_m = \int H^m\, P(H)\mathrm{d}H \tag{5}$$

As we have shown [1], we can obtain a set of the enthalpy moments directly from the temperature dependence of the heat capacity, specifically, from the constants a, b and c of Eq. (3). Given the expansion of the heat capacity through the term in ΔT^2 given in Eq. (2) is enough information to experimentally obtain the first four enthalpy moments. Given just the value of C_p at T_r is enough information to obtain two enthalpy

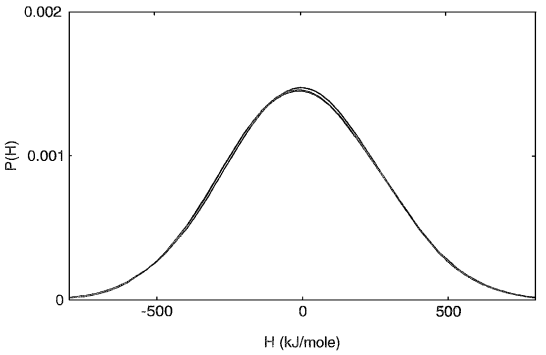

Fig. 3. The enthalpy probability distribution, $P(H)$, as a function of the enthalpy in units of kJ mol^{-1} for $tRNA^{Phe}$ at the temperature of the maximum in the heat capacity (53.7 °C) as shown in the broad curve in Fig. 1 (which is repeated in Fig. 2). There are three curves shown giving the results of using two, four, and six moments, respectively, to calculate $P(H)$. In this case the three results are essentially identical.

moments, while an expansion of C_p that is quadratic in ΔT yields six such moments.

Given a finite set of enthalpy moments, we then use the maximum-entropy method [1,7] to obtain an approximation to the function $P(H)$. In this method, a general distribution function $P(x)$ is expressed as follows:

$$P(x) = \exp[-g(x)] \tag{6}$$

where

$$g(x) = \sum_{m=0}^{n} x^m \lambda_m \tag{7}$$

Specifically, the method involves a technique whereby we take a set of moments, the H_m, and convert these into a set of parameters, the λ_m given in Eq. (7). The numerical technique to obtain the λ values from the moments involves a non-linear iteration procedure that is simple and quick. If we have the values of n moments, we can then calculate the λ parameters through λ_n (the parameter λ_o acts as a normalization constant). The more moments we have, the more λ parameters in Eq. (7) that can be calculated, and the closer the approximate distribution thus obtained will be to the actual distribution. If we have only two moments, then the distribution function obtained is of the classic Gaussian form. If we have four moments, then we can resolve two peaks in the distribution function; this bimodal behavior is observed in $P(H)$ for many proteins [2]. We can observe that for the tRNA molecules treated in the present work the distribution functions converge very rapidly to a limiting form as the number of moments used is increased.

As an example of the construction of the distribution function $P(H)$, we show the results obtained when we pick the temperature-expansion center for $tRNA^{Phe}$ at the peak in the $C_p(T)$ function that is shown in Fig. 2. Expanding $C_p(T)$ about this temperature in a quadratic in ΔT gives six moments of the enthalpy distribution at the given temperature. Using the maximum-entropy method, we then obtain $P(H)$ using successively two, four and six moments. The results of this calculation are shown in Fig. 3. It is evident that the results for the three cases are almost superimposable, indicating that in this case the Gaussian form of the distribution function is quite accurate, which is in contrast to the behavior found in many proteins, where the four-moment distribution is qualitatively different from the two-moment distribution [2].

We note that for the case where we use only two moments, the enthalpy probability distribution function can be given without using the maximum-entropy method. The result is:

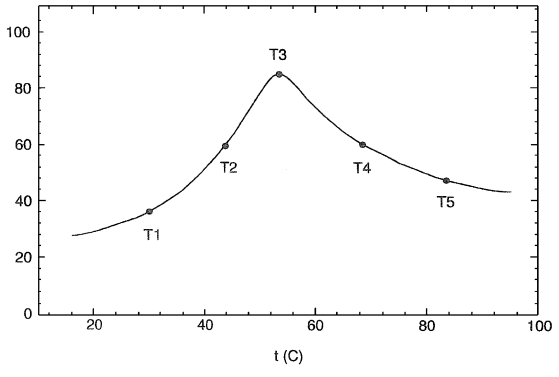

Fig. 4. The heat capacity (in units of kJ mol^{-1} K^{-1}) as a function of the centigrade temperature of $tRNA^{Phe}$ for the case of 150 mM NaCl showing the five temperature-expansion centers.

$$P(H)=\frac{1}{\sigma\sqrt{2\pi}}\exp\left[-(H-H_1)^2/2\sigma^2\right] \quad (8)$$

where H_1 is the average enthalpy at temperature T. The quantity σ is given by either of the two forms given below:

$$\sigma=\sqrt{RT^2C_p(T)}=\sqrt{H_2-H_1^2} \quad (9)$$

where R is the gas constant in appropriate units and H_2 is the second moment. The result of Eq. (8) applies when the range of H is not restricted, that is when there are neither lower or upper bounds to H. In that case, Eq. (8) gives the same result as the maximum-entropy method. If there is a lower bound (for example, in the distribution for the kinetic energy of an ideal gas where the energy must be greater than zero), then we must use the maximum-entropy method [1].

3. Free energy distributions

Given an approximate enthalpy distribution function, we can then define a corresponding free energy as the potential for $P(H)$ as follows:

$$P(H)=\exp\left[-G(H)/RT\right]/\exp\left[-G/RT\right] \quad (10)$$

where

$$\exp\left[-G/RT\right]=\int\exp\left[-G(H)/RT\right]\mathrm{d}H \quad (11)$$

The quantity G is the usual Gibbs free energy and $G(H)$ is that part of G that corresponds to a particular value of the enthalpy.

To understand $G(H)$ further, it is useful to use the analogy with the Helmholtz free energy for a single molecule expressed as a sum over all energy states (the canonical partition function):

$$\exp\left[-A/RT\right]=\sum\nolimits_E\Omega(E)\exp\left[-E/RT\right] \quad (12)$$

The quantity $\Omega(E)$ gives the number of ways a fixed energy E can be arranged in the molecule, and it is important to note that $\Omega(E)$ is independent of temperature. We then rewrite Eq. (12) as:

$$\exp\left[-A/RT\right]=\sum\nolimits_E\exp\left[-A(E)/RT\right] \quad (13)$$

where

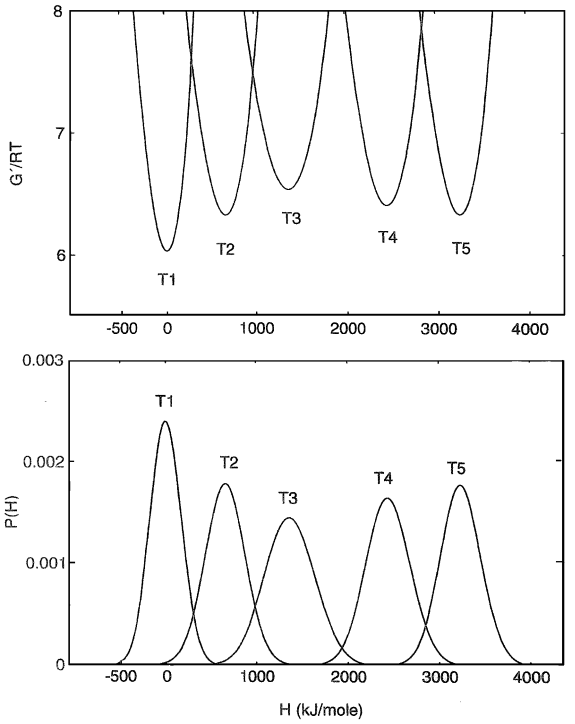

Fig. 5. The lower graph shows the enthalpy distribution function, $P(H)$, as a function of the enthalpy in units of kJ mol^{-1} evaluated at the five temperatures indicated in Fig. 4. The upper graph gives the corresponding function G'/RT as given by Eq. (19) for each of the five distributions in the lower graph.

$$A(E)=E-RT\ln\Omega(E) \quad (14)$$

What we have done in Eq. (13) and Eq. (14) is to write the total free energy, A, in terms of a quantity $A(E)$ referring to a particular value of the energy. We are thus using the partition function of statistical mechanics to introduce the concept of $A(E)$, but it is important to emphasize that we do not require a specific model of the system in order to do this.

The quantity $G(H)$ used in Eq. (10) and Eq. (11) is the analog of $A(E)$ used in Eq. (14), that is:

$$G(H)=H-TS(H) \quad (15)$$

At constant pressure, G and H replace A and E, the appropriate thermodynamic functions for the condition of constant volume (for condensed sys-

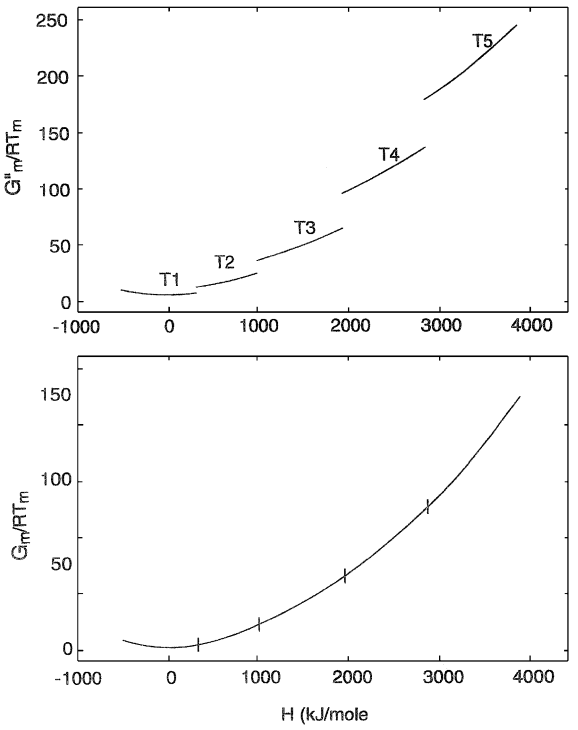

Fig. 6. The upper graph shows five sections of the function G''/RT_m obtained from the five sections of G'/RT shown in Fig. 5 and scaled to the same reference temperature, T_m, using Eq. (22). The lower graph shows the function G_m/RT_m formed by eliminating the jumps between the pieces of the function in the upper graph. The vertical lines indicate the position of the joints between the original pieces.

tems there is little difference between G and A and between E and H). Since we consider H a continuous variable, the sum in Eq. (13) is replaced by an integral over all values of H in Eq. (11). An explicit example of the use of Eq. (12), Eq. (13) and Eq. (14) and moments to calculate probability distributions is given elsewhere [1].

The quantity of interest in Eq. (10) and Eq. (11) is $G(H)/RT$, which we can form from $G(H)$ given in Eq. (15):

$$G(H)/RT = H/RT - S(H)/R \tag{16}$$

We then introduce a special version of Eq. (16) in which the appropriate quantities are evaluated at a reference temperature, which we designate as T_m:

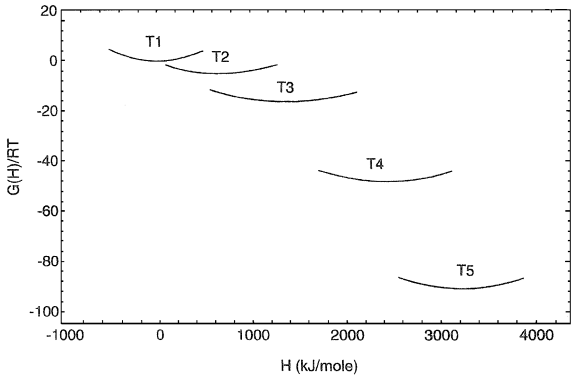

Fig. 7. The function $G(H)/RT$ as a function of the enthalpy in kJ mol^{-1} at the five temperatures shown in Fig. 4 as obtained from the reference function G_m/RT_m using Eq. (18).

$$G_m(H)/RT_m = H/RT_m - S(H)/R \tag{17}$$

The quantity $S(H)$ that appears in both Eq. (16) and Eq. (17) is not a function of temperature, since it is the analog of $R\ln\,\Omega(E)$ in Eq. (12) and Eq. (14). The total entropy, for example as given by using the total A of Eq. (12), is of course temperature-dependent, but $R\ln\,\Omega(E)$ is not. We can then subtract Eq. (16) from Eq. (17) and $S(H)$ cancels, giving the important relation:

$$G(H)/RT = G_m(H)/RT_m - \frac{H}{R}\left(\frac{1}{T_m} - \frac{1}{T}\right) \tag{18}$$

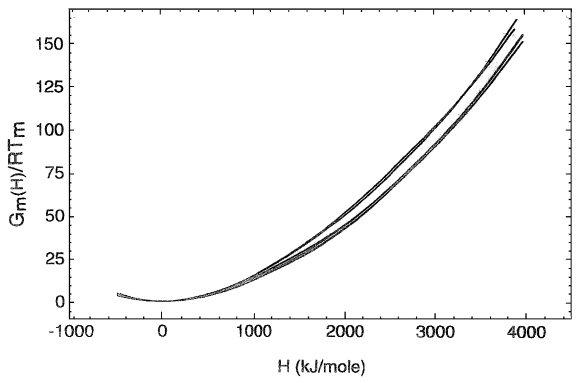

Fig. 8. The reference functions G_m/RT_m as a function of the enthalpy in kJ mol^{-1} for the six tRNAs illustrated in Fig. 2. The reference temperature is taken as 30 °C for each. The zero of free energy is taken as $G_m = 0$ at $H = 0$.

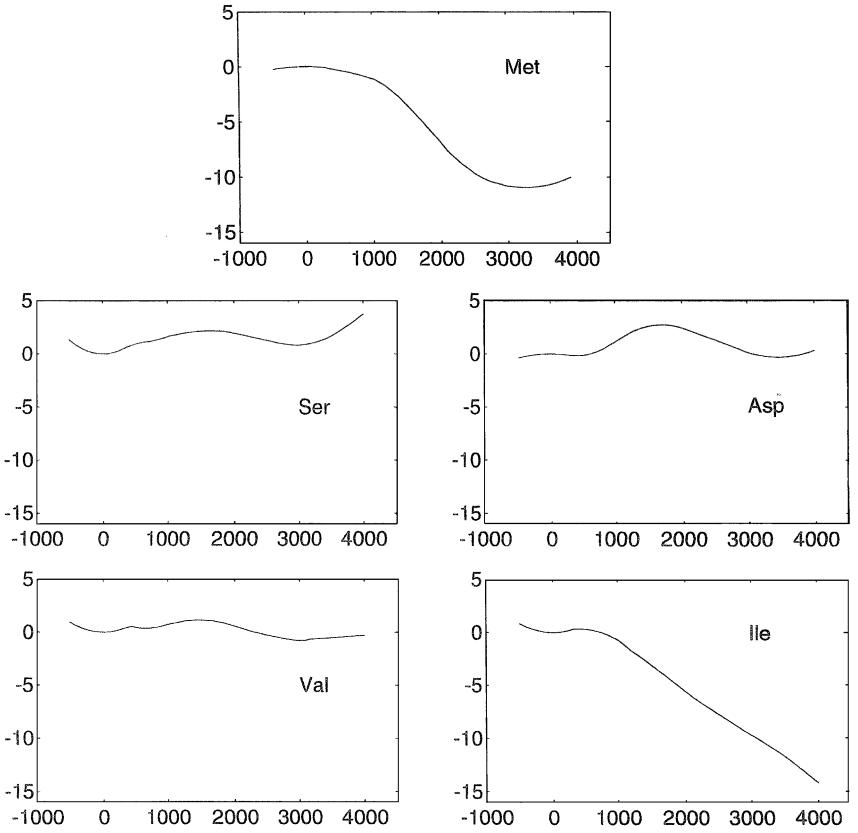

Fig. 9. The difference, as defined in Eq. (25) between the reference function G_m/RT_m for $tRNA^{Phe}$ and the other amino acids considered as a function of the enthalpy in kJ mol^{-1}.

This gives the function $G(H)$ at an arbitrary temperature in terms of the function $G_m(H)$ at the reference temperature T_m. Thus, if we know the reference function $G_m(H)$, we can then calculate the thermodynamics and the distribution functions at all other temperatures. Our task in the present paper is to obtain and compare the $G_m(H)$ functions for a set of tRNAs.

We begin our calculation of $G(H)$ using the relation between $P(H)$ and $G(H)$ given in Eq. (10). We assume that we have obtained a set of enthalpy moments from an expansion of $C_p(T)$ in powers of ΔT and, using the maximum-entropy method, have converted the moments into an approximate distribution function $P(H)$. Taking the logarithm of $P(H)$, we have from Eq. (10):

$$G'(H)/RT = -\ln P(H) = G(H)/RT - G/RT \qquad (19)$$

The quantities $G'(H)$ and $G(H)$ are the same to within a temperature-dependent constant, G/RT. We illustrate the construction and nature of the functions $G'(H)/RT$ using $tRNA^{Phe}$ as an example, since from Fig. 2 the behavior of $C_p(T)$ for this system is the simplest of the six tRNAs considered. In Fig. 4 we repeat the graph of $C_p(T)$ for $tRNA^{Phe}$, indicating with solid dots five different temperature values to be used as expansion centers. The five temperature values chosen are: $T=30$, 44, 53.7, 68.7 and 83.7 °C. At each temperature center we construct $P(H)$ and then, using Eq. (19), calculate $G'(H)/RT$.

The $P(H)$ and $G'(H)/RT$ functions thus obtained for $tRNA^{Phe}$ at each of the five temperatures indicated in Fig. 4 are shown in Fig. 5. In Fig. 3 we showed that, for $tRNA^{Phe}$ at T_3 (the

temperature of the maximum in C_p), the function $P(H)$ was approximated very well by the form constructed from only two moments, with the result that the $P(H)$ functions for this system are approximately Gaussian. The $P(H)$ functions can be quite asymmetric or even bimodal, so this need not be true in general. For the present example, the approximately Gaussian shape of $P(H)$ translates into the simple behavior of $G'(H)/RT$ shown in Fig. 5, in which the curves are approximately symmetric about the minimum, each containing only a single minimum corresponding to the single maximum in $P(H)$. We note that as the temperature is increased from T_1 to T_5 the maximum in $P(H)$ simply moves to a higher value of H, and that there is no qualitative feature that is different with respect to the function at T_3, the temperature of the heat capacity maximum.

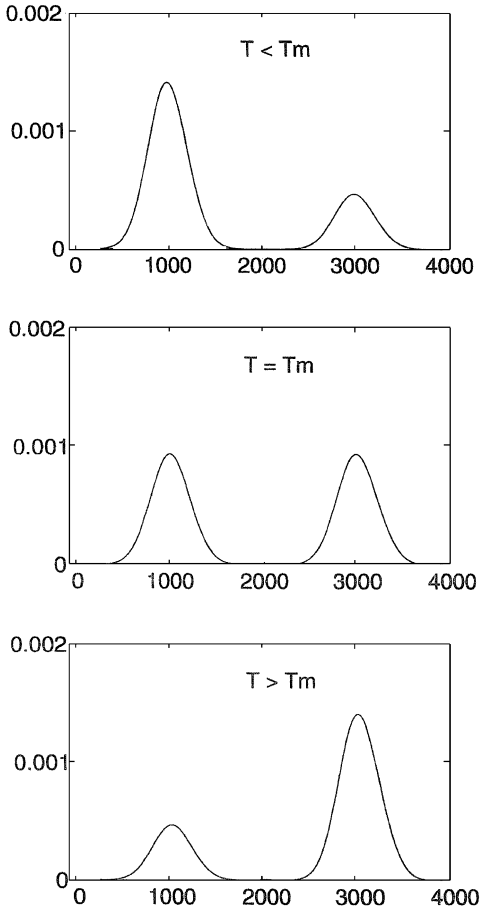

Fig. 10. Schematic probability distribution, $P(H)$, as a function of the enthalpy for the case where the distribution is bimodal reflecting the existence of two distinct species (native and unfolded). As the temperature is increased, the probability of the native species decreases and the probability of the unfolded species increases.

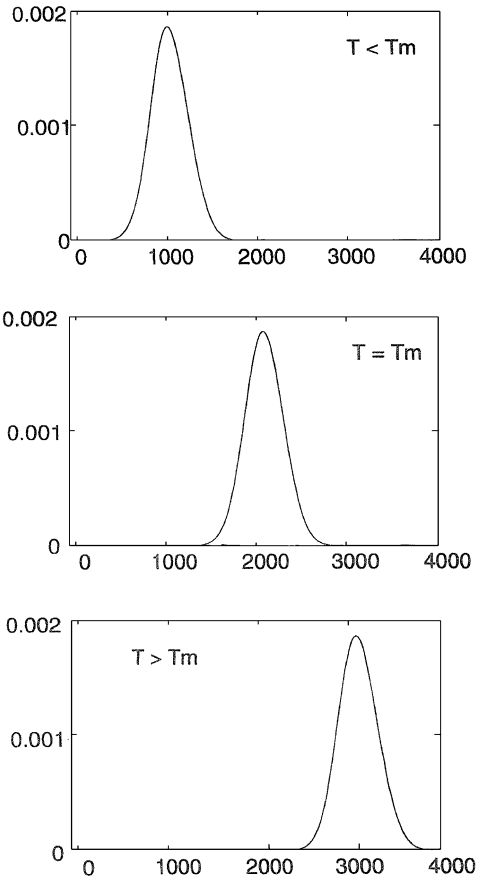

Fig. 11. Schematic probability distribution, $P(H)$, as a function of the enthalpy for the case where the distribution at all temperatures is unimodal and simply shifts the maximum to higher values of the enthalpy as the temperature is increased.

An important feature illustrated by the curves shown in Fig. 5 is that by choosing a range of temperature expansion centers, as illustrated in Fig. 4, we then cover a wide range of H values, as shown by the H scale in Fig. 5. In particular, the five $P(H)$ functions shown overlap one another, and thus leave no gaps in the values of H covered. The function $G'(H)/RT$ is thus sensitive

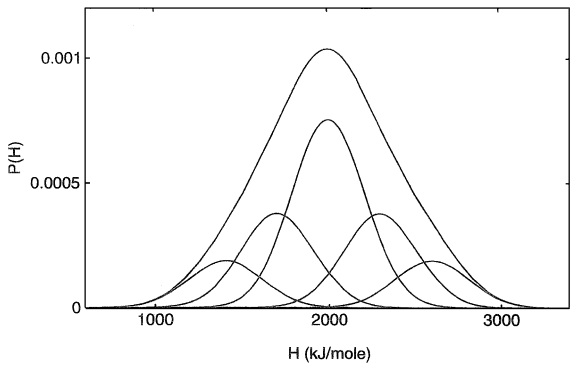

Fig. 12. A schematic illustration of a probability distribution, $P(H)$, as a function of the enthalpy for the case where the system has a number of significant structures, each with a fairly broad probability distribution. In this case the sum of the individual curves yields a unimodal overall distribution.

to the H dependence of the free energy at a particular temperature and range of H values. The importance of Eq. (18) is that the H dependence of $G'(H)/RT$ at the temperature indicated can be shifted to any temperature (keeping the range of H fixed). Thus, by using a range of temperatures we can construct a $G'(H)/RT$ function at any temperature that is accurate over a very wide range of H values (in the present case, the whole H scale shown in Fig. 5).

Thus, taking T_m as a general reference temperature, we can use Eq. (18) to relate $G'(H)/RT$ to G'_m/RT_m:

$$G'_m(H)/RT_m = G'(H)/RT + \frac{H}{R} \times \left(\frac{1}{T_m} - \frac{1}{T}\right) + C(T,T_m) \qquad (20)$$

where

$$C(T,T_m) = G/RT - G_m/RT_m \qquad (21)$$

We then define a version of Eq. (20) that deletes the constant C:

$$G''_m(H)/RT_m = G'(H)/RT + \frac{H}{R}\left(\frac{1}{T_m} - \frac{1}{T}\right) \qquad (22)$$

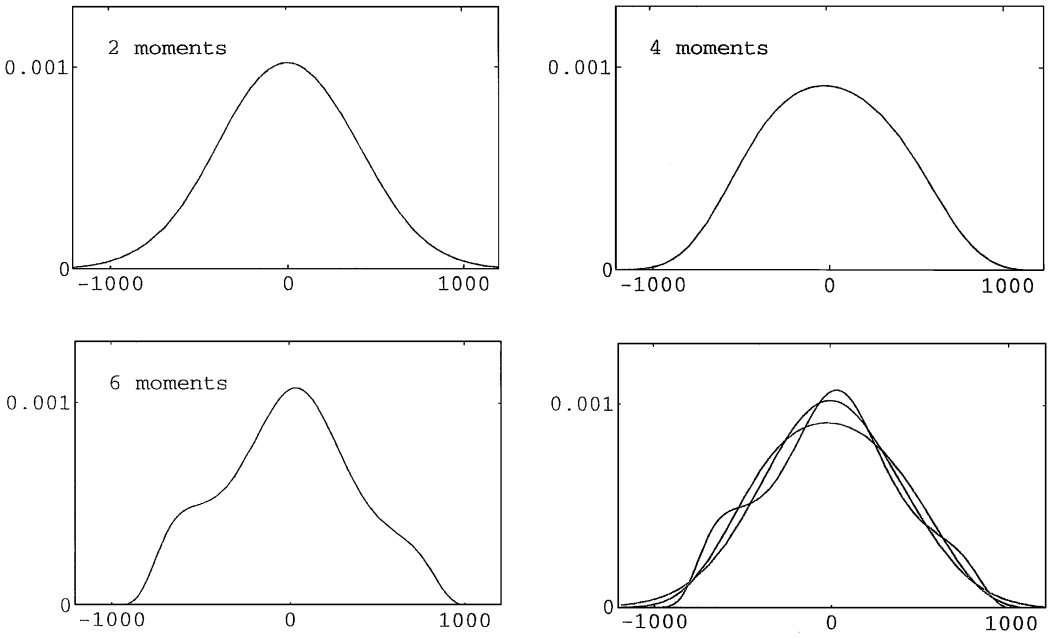

Fig. 13. The probability distribution, $P(H)$, as a function of enthalpy in kJ mol^{-1} for the middle peak in Fig. 1 for tRNA^{Phe}; the expansion temperature is the temperature of the maximum in the heat capacity, 67.4 °C. Shown are the distributions obtained using two, four and six moments; the final graph shows the three curves plotted together.

We can now construct G''_mover a very broad range of H using the $G'(H)$ given in Fig. 5 at five different temperatures, and relating them all to T_m using Eq. (22). The result of this operation is shown in the upper graph in Fig. 6. Each of the five pieces of the curve shown represents one of the G' functions shown in Fig. 5 transformed by Eq. (22). It is evident that between each segment there is a jump discontinuity, which arises because the normalizing constants, $C(T,T_m)$ in Eq. (20), were not used. We can accomplish the equivalent of using the correct constants simply by eliminating the jump discontinuities in the upper graph, giving the result shown in the lower graph in Fig. 6. It is now evident that we have a smooth, continuous curve representing $G_m(H)/RT_m$ over a very wide range of H values. We take the reference point for the constant C as T_m, and hence set this quantity equal to zero for G_m. We thus delete the prime on G_m.

Given the complete function $G_m(H)$, we can then construct $G(H)$ at any other temperature [not just the five temperature values used in the construction of $G_m(H)$] using Eq. (18). It is evident in the lower graph in Fig. 6 that G_m/RT_m for $T_m=$ 30 °C has a shallow minimum at $H=0$, which means that the most probable value of H at this temperature is $H=0$ [as shown by the $P(H)$ curve for T_1 in Fig. 5]. Using Eq. (18) to construct $G(H)/RT$ for higher temperatures has the effect of successively moving the position of the minimum in $G(H)/RT$ to higher values of H (again, as illustrated in Fig. 5). The portions of $G(H)/RT$ in the neighborhood of the respective minima for the five temperature values we have already used are shown in Fig. 7 (we of course are not restricted to these values of the temperature). We again emphasize that all of the curves shown come from G_m/RT_m shown in the lower graph in Fig. 6 and transformed to higher temperature values using Eq. (18). The $G(H)/RT$ curves shown in Fig. 7 then translate directly to the $P(H)$ curves by the use of Eq. (10), with the normalization condition given by Eq. (11); in fact, the free energy curves shown in Fig. 5 are the normalized versions of the free energy curves shown in Fig. 7.

For completeness, we note that, given $G(H)$, or equivalently $P(H)$, at any temperature, we can calculate C_p at the same temperature, thus coming back to the original C_p data. Given $G(H)$, we have:

$$\langle H\rangle = \int H\exp\left[-G(H)/RT\right]\,\mathrm{d}H \Big/ \int \exp\left[-G(H)/RT\right]\,\mathrm{d}H$$

$$\langle H^2\rangle = \int H^2\exp\left[-G(H)/RT\right]\mathrm{d}H \Big/ \int \exp\left[-G(H)/RT\right]\,\mathrm{d}H \qquad (23)$$

Then

$$C_p = \frac{\partial\langle H\rangle}{\partial T} = \left[\langle H^2\rangle - \langle H\rangle^2\right]/RT^2 \qquad (24)$$

Since $P(H)$ was constructed using at least the first two moments of the enthalpy distribution [i.e. $P(H)$ gives at least the first two moments of the enthalpy distribution exactly], then Eq. (23) and Eq. (24) give the original experimental value of C_p exactly.

4. Comparison of the thermal behavior of the tRNAs

We have carried out a similar analysis for each of the six tRNAs shown in Fig. 2 using the same T_m (30 °C) for each and taking the zero of $G_m(H)/RT_m$ at $H=0$ for T_m. The reference function $G_m(H)/RT_m$ for all six of the tRNAs is shown in Fig. 8. It is evident on the scale of that figure that the reference free-energy distributions for all of these molecules are very similar. Yet it is clear from the behavior of $C_p(T)$ for these molecules shown in Fig. 2 that there are differences in the thermal behavior. This is best shown by plotting the difference in the G_m functions. Taking $tRNA^{Phe}$ (the simplest case) as a reference, we define the difference function for a general amino acid X:

$$\Delta G_m[\mathrm{X}] = G_m[\mathrm{Phe}] - G_m[\mathrm{X}] \qquad (25)$$

These functions are shown in Fig. 9, and it is now evident that there are indeed marked differences in the behavior of this function for different molecules.

The general behavior of $P(H)$ found for the tRNAs is contrasted with that found in many proteins [5]. Fig. 10 qualitatively shows the pattern for the case in which there is a bimodal $P(H)$, indicating native and unfolded forms; the two peaks change in relative intensity as a function of temperature, shifting from one to the other. This is in contrast to the behavior typical of the tRNAs as shown in Fig. 11, where $P(H)$ has a single peak at all temperature values, the maximum simply shifting to higher enthalpy values as the temperature is increased.

The probability distribution for tRNAs we find, as shown in the lower half of Fig. 5 for $tRNA^{Phe}$, is similar to that shown in Fig. 11. We note that this does not mean that there is a population of more or less distinct structures. This is illustrated in Fig. 12, where five separate peaks represent five species. Each peak is relatively broad, and when they are added together the result is an overall unimodal peak. By changing the relative intensity of each peak, a migrating peak can then be obtained, as shown in Fig. 5.

Finally, we return to a consideration of the other peaks in Fig. 1. As mentioned earlier, the problem with treating the sharper peaks in Fig. 1 is that it is very difficult to obtain accurately the experimental data from the published graphs. Here we treat the middle peak and expand the heat capacity about the temperature of the maximum. In Fig. 13 we show the $P(H)$ distribution functions obtained from these data using two, four and six moments. In this case, differences are observed in the distribution functions obtained using different numbers of moments. In particular, the distribution function obtained using six moments exhibits notable shoulders. However, when plotted together, as shown in Fig. 13, the three curves are approximately similar.

References

[1] D. Poland, Maximum-entropy calculation of energy distributions, J. Chem. Phys. 112 (2000) 6554–6562.
[2] D. Poland, Enthalpy distributions in proteins, Biopolymers 58 (2001) 89–105.
[3] G.I. Makhatadze, P.L. Privalov, Energetics of protein structure, Adv. Protein Chem. 47 (1995) 307–425.
[4] D. Poland, Densities of states in gases, liquids and solids, J. Chem. Phys. 113 (2000) 9930–9939.
[5] D. Poland, Free energy distributions in proteins, Proteins: Struct. Funct. Genet. 45 (2001) 325–336.
[6] P.L. Privalov, V.V. Filimonov, Thermodynamic analysis of transfer RNA unfolding, J. Mol. Biol. 122 (1978) 447–464.
[7] A. Tagliani, On the application of maximum entropy to the moments problem, J. Math. Phys. 34 (1993) 326–337.